From the DEPARTMENT OF CLINICAL NEUROSCIENCE,
PSYCHIATRY SECTION
Karolinska Institutet, Stockholm, Sweden

IN VIVO QUANTIFICATION OF EXTRASTRIATAL DOPAMINE D2 RECEPTORS IN THE HUMAN BRAIN

Hans Olsson

Stockholm 2005

Published and printed by Karolinska University Press
Box 200, SE-171 77 Stockholm, Sweden

ISBN 91-7140-290-X

ABSTRACT

The dopamine D2 receptor subtype attracts considerable attention in research on the patophysiology and drug treatment of several neuropsychiatric disorders, such as schizophrenia and Parkinson's disease. The brain imaging technology Positron Emission Tomography (PET) has since long allowed for reliable quantification of the high density of dopamine D2 receptors in large brain structures such as the neo-striatum. Several extrastriatal brain regions with low dopamine D2 receptor density are of central interest in current hypotheses on the role of dopaminergic neurotransmission in neuropsychiatric disorders. New methodologies are required for this purpose.

The radioligand [^{11}C]FLB 457 has the very high affinity of 20 pM for dopamine D2 receptors *in vitro* and allows for visualization of binding to the minute concentrations of dopamine D2 receptors in extrastriatal regions in the human brain *in vivo*. The overall aim of the present thesis was to examine and compare methodologies for quantification of regional [^{11}C]FLB 457 binding in the living human brain.

Altogether ten control subjects participated in twenty-six PET measurements. To obtain absolute values for dopamine D2 receptor density and affinity, each subject participated in two to three PET measurements with different mass of radioligand injected. A metabolite corrected arterial input function was used in standard compartment model analyses and the cerebellum was evaluated as reference region in simplified quantitative approaches including a Scatchard analysis. Due to the lack of a simple analytical solution for the non-linear two-tissue compartment model, simulations were performed to understand the temporal behavior of radioligand binding.

[^{11}C]FLB 457 binding to extrastriatal regions could be described by the two-tissue compartment model and the rank order of regional binding potential (*BP*) values was consistent with the rank order reported in binding studies on human brain tissue postmortem. Experimental data and simulation studies showed that the time to reach peak of specific radioligand binding is dependent on regional receptor density and varied between 39 and 63 minutes due to the several-fold difference in dopamine D2 receptor density across brain regions. Ratio methods underestimate drug-induced occupancy particularly in regions with high receptor density whereas the Simplified Reference Tissue Model (SRTM) yielded valid estimations. However, the *BP* obtained for the striatum, i.e. the region with highest density, was underestimated since ^{11}C-labeled FLB 457 only allows for an acquisition time of about 1 hour. The regional receptor density (B_{max}) values obtained by Scatchard analysis were close to the *in vitro* values given in the literature. The affinity was about 10 to 20 times lower *in vivo* indicating that the free radioligand concentration in the extracellular space represents only a minor fraction of non-displaceable radioligand in brain. With regard to the cerebellum as reference region for non-displaceable binding it can not be excluded that [^{11}C]FLB 457 is sensitive to the minute receptor density of dopamine D2 receptors in this region. Theoretical considerations illustrated by a simulation approach showed that the emerging concept of "receptor occupancy half-life" is not supported by theory. Instead, initial receptor occupancy and the time-constant for drug clearance in plasma can be used in clinical studies to estimate the net-dissociation of a drug from the

receptors. Finally, it was shown that [^{11}C]FLB 457 can be used to visualize and quantify binding in the non-diseased human pituitary. The calculated receptor density is consistent with *in vitro* values.

The thesis work shows that the PET radioligand [^{11}C]FLB 457 can be used *in vivo* in the human brain to obtain valid estimates of binding parameters in extrastriatal brain regions containing dopamine D2 receptors as well as in the pituitary gland. Due to the short half-life of carbon-11, [^{11}C]FLB 457 cannot be used in regions with high receptor density, such as the striatum. The methodology can be applied in clinical studies on hypotheses regarding the role of the extrastriatal dopamine systems in neuropsychiatric disorders.

LIST OF PUBLICATIONS

I. Olsson, H., C. Halldin, C. G. Swahn and L. Farde (1999). Quantification of [^{11}C]FLB 457 binding to extrastriatal dopamine receptors in the human brain. *J Cereb Blood Flow Metab 19(10): 1164-73*

II. Olsson, H. and L. Farde (2001). Potentials and pitfalls using high affinity radioligands in PET and SPET determinations on regional drug induced D2 receptor occupancy – a simulation study based on experimental data. *Neuroimage 14(4): 936-45*

III. Olsson, H., C. Halldin and L. Farde (2004). Differentiation of extrastriatal dopamine D2 receptor density and affinity in the human brain using PET. *Neuroimage 22(2): 794-803*

IV. Olsson, H. and Farde, L. (2005). Receptor occupancy half-life – a meaningless concept. *Int J Neuropsychopharmacol 8(1):141-2.*

V. Olsson, H., Halldin, C. and Farde, L. Visualization and quantification of dopamine D2 receptors in the human pituitary using PET and [^{11}C]FLB 457. *Manuscript*

CONTENTS

LIST OF ABBREVIATIONS

ADHD	attention deficit/hyperactive disorder
AUC	area under curve
BBB	blood-brain-barrier
B_{max}	receptor density (nM)
BP	binding potential
DA	dopamine
EPS	extrapyramidal side-effects
HPLC	high performance liquid chromatography
K_1	rate constant for in-flux of ligand over BBB (min^{-1})
k_2	rate constant for out-flux of ligand over BBB (min^{-1})
k_3	association rate constant (min^{-1})
k_4	dissociation rate constant (min^{-1})
K_D	equilibrium dissociation constant (nM)
k_{off}	unimolecular dissociation rate constant (min^{-1})
k_{on}	bimoluecular association rate constant (ml $pmol^{-1}$ min^{-1})
MRI	magnetic resonance imaging
mRNA	messenger RNA
PET	positron emission tomography
pM	pico-molar
PRL	prolactin
ROI	region of interest
SA	specific radioactivity (Ci $mmol^{-1}$)
SN	substantia nigra
SPET	single photon emission tomography
SPM	statistical parametric mapping
SRTM	simplified reference tissue model
TAC	time activity curve
VTA	ventral tegmental area

1 INTRODUCTION

Dopamine (DA) is one of the first neurotransmitters in the phylogenesis and has since long been known to be involved in motor- and endocrine functions in brain. More recent research has established a role for DA in cognition and higher brain functions. Disturbances in the dopaminergic transmission system have been implicated in neuropsychiatric disorders, such as schizophrenia, Parkinson's disease and ADHD. The system has been a target for intense research with positron emission tomography (PET) for some twenty years. However, this non-invasive technique has until now only allowed for visualization and quantification of dopamine receptors in large central structures, such as the basal ganglia. New radioligands with high affinity for dopamine receptors has been developed for detailed examination of the dopaminergic system throughout the whole brain, i.e. also in small regions with sparse innervations. Due to their high affinity, these ligands provide particular challenges with regard to quantification of binding in the human brain *in vivo*. One of the new ligands is the substituted benzamide [^{11}C]FLB 457. The present thesis aims at quantitative modeling of [^{11}C]FLB 457 binding and examination of its' potential for detailed studies of dopamine receptors in the healthy and diseased human brain *in vivo*.

1.1 DOPAMINERGIC SYSTEMS IN THE BRAIN

In the human brain the DA system can be divided in four parts or pathways (figure 1-1). *(i)* The nigrostriatal pathway originates in substantia nigra (SN) in the brainstem and provides dense innervations to the dorsal striatum (nucleus caudatus and putamen). This pathway has a role in control of motor function and is also thought to play a role in the timing and synchronization of cognitive functions. *(ii)* The mesocortical pathway, originating from the ventral tegmental area (VTA) in the brainstem and ending in the neo-cortex has been proposed to be involved in learning and memory. *(iii)* The mesolimbic pathway is another dopaminergic pathway originating in VTA and reaches the ventral striatum and limbic cortical regions. The mesolimbic pathway has been implicated in motivated behavior and emotions. The fourth pathway, *(iv)* the tuberoinfundibular pathway, descends from periventricular hypothalamus to the median eminence of hypothalamus where DA is released into the hypothalamic-hypophysial portal blood circulation and eventually reaches the pituitary. Here DA inhibits prolactin release from the lactotrophs in the anterior endocrine part of the gland.

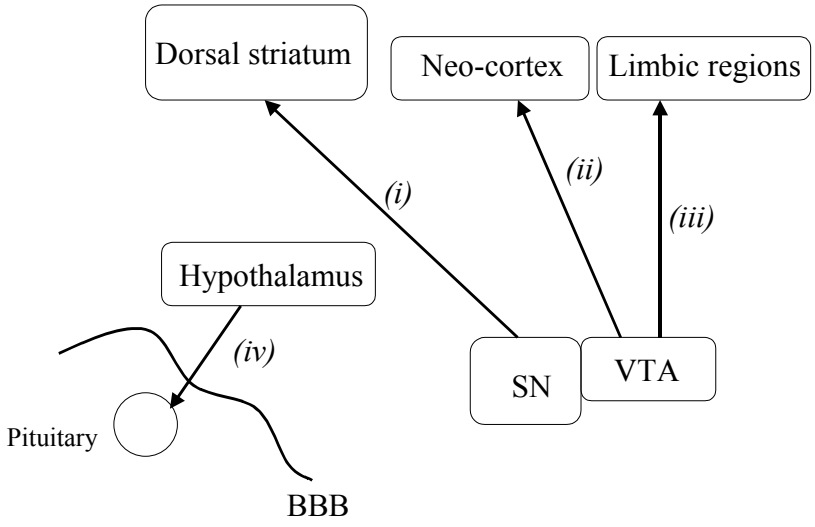

Figure 1-1. Major dopaminergic pathways. *(i)* The nigrostriatal pathway, *(ii)* the mesocortical pathway, *(iii)* the mesolimbic pathway and *(iv)* the tuberoinfundibular pathway. SN = substantia nigra, VTA = ventral tegmental area, BBB = blood-brain barrier.

1.2 DOPAMINE RECEPTOR SUBTYPES

Dopamine exerts its actions by binding to membrane bound receptor proteins. There are at least five different dopamine receptor subtypes in the human brain. The receptors activate or inhibit the cAMP pathway and modulate intracellular Ca^{2+} levels. They are usually divided into two families based on biochemical and pharmacological properties. The first family is denoted D1-like receptors and consists of the D1 and D5 subtype. At binding of DA, these receptors activate the intracellular cAMP pathway. The family of D2 receptors, consists of the D2, D3 and D4 subtype. They inhibits the formation of cAMP (Missale et al. 1998; Vallone et al. 2000).

The D2 subtype is expressed in a short and a long isoform but no obvious functional difference between the two isoforms have been demonstrated so far (Malmberg et al. 1993; Missale et al. 1998). Both variants share the same distribution pattern and pharmacological profile, although the shorter form seems less abundantly expressed.

The DA receptors have two inter-convertible affinity states, each reflecting a conformation of the receptor protein (Lefkowitz et al. 1993). The affinity states are defined by agonists like DA that differentiate between two affinity states (high and low) whereas antagonists bind with the same affinity regardless of state. It has been estimated that about 70% of dopamine D2 receptors in baboons are configured in a state of high affinity for agonists *in vivo* (Narendran et al. 2004).

Available PET radioligands for dopamine receptors discriminate between the D1 and D2-like receptors. However, most of the ligands are not selective for members of the same subfamily (Vallone et al. 2000). Moreover, most radioligands developed so far

are antagonists that do not differentiate between the low and high affinity state. More recently promising agonist radioligands have been developed for the D2 subtype (Finnema et al. 2005).

1.3 REGIONAL EXPRESSION OF DOPAMINE D2-LIKE RECEPTORS

The regional concentration of dopamine and D2-like dopamine receptors is highest in the striatum and the substantia nigra. However, several extrastriatal regions express dopamine receptors albeit in much lower concentrations (Kessler et al. 1993; Hall et al. 1996; Hurd et al. 2001). The D2-like receptors are localized both post- and pre-synaptically, whereas the D1-like family is exclusively postsynaptic (Vallone et al. 2000).

Brain region	Receptor density (*pmol/g tissue*)
Putamen	16.6
Caudate	16.5
Nucleus accumbens	7.2
Globus pallidus	7.0
Thalamus	0.7-1.0
Amygdala	0.9
Laterar temporal cortex	0.3
Anterior cinguli	0.3
Middle frontal gyrus	0.2
Pituitary	1.3

Table 1-1 Regional dopamine D2 receptor density in post mortem human brain specimens (from Kessler et al. 1993).

1.3.1 Neo-striatum

The dopamine D2 receptor subtype is expressed in high concentration in the caudate nucleus and the putamen. The D3 subtype is rather highly expressed in the accumbens whereas the density is low in the dorsal striatum (Meador-Woodruff et al. 1997; Missale et al. 1998; Gurevich and Joyce 1999). The striatal levels of dopamine D4 receptors are low.

1.3.2 Thalamus

Autoradiographic studies have shown relatively high concentration of dopamine D2-like receptors in the human thalamus. Binding is not uniform but concentrated to intralaminar and midline thalamic nuclei whereas moderate receptor densities have been found in the mediodorsal and anterior nuclei and the pulvinar (Kessler et al. 1993; Rieck et al. 2004). Also in situ hybridization supports heterogeneous distribution of the D2 receptor subtype in the thalamus with high concentration of mRNA in regions expressing the D2 receptor protein (Gurevich and Joyce 1999).

1.3.3 Cortex

The D1-like receptors are relatively highly expressed in the neo-cortex whereas the density of D2-like receptor is low. The density varies between cortical regions. Highest density has been shown in temporal cortex, insular cortex, anterior cingulate and frontal cortex in named order (table 1-1). The receptor density in these regions is approximately 0.2 to 1.5% of that in striatum (Kessler et al. 1993; Hall et al. 1996; Hurd et al. 2001).

1.3.4 Cerebellum

Very low values for dopamine D2-like receptor density has been demonstrated for the cerebellar cortex (Hall et al. 1996). The receptor density has been calculated to 0.1% of that found in striatum. Furthermore, in situ hybridization for dopamine D2 receptor mRNA in the cerebellar cortex has shown a signal above background (Hurd et al. 2001).

1.3.5 Other brain structures

Relatively high dopamine D2-like receptor binding has been shown in the lateral globus pallidus but virtually no mRNA for the receptor can be demonstrated in this region (Kessler et al. 1993; Hall et al. 1996; Gurevich and Joyce 1999; Hurd et al. 2001). It has been suggested that the D2 receptors in globus pallidus stem from striopallidal projection neurons (Hurd et al. 2001).

Hypothalamus, septum, the amygdala complex, substantia nigra, superior colliculus, claustrum and hippocampus are regions that have been shown to have relatively high dopamine D2 receptor density, i.e. in the rage of 2 to 30% of that found in the striatum (Hall et al. 1996).

1.3.6 The pituitary

The pituitary is an endocrine gland located outside the blood-brain barrier (Ganong 2003). Dopamine D2-receptors in the pituitary are stimulated by dopamine, which is released into the hypothalamic-hypophysial portal system from neurons originating in the hypothalamus (the tuberoinfundibular pathway). DA stimulation inhibits prolactin (PRL) release from the lactotrophs in the anterior part of the gland.

1.4 POSITRON EMISSION TOMOGRAPHY (PET)

Positron emission tomography is a non-invasive imaging technique developed in the 1970s. The technique uses molecules that are labeled with short-lived radioisotopes that are injected intravenously. New molecules, such as potential drugs, can then be traced in the brain and its' kinetic properties and anatomical distribution can be determined. The demonstration of quantitative relationships between drug binding *in vivo* and drug effects in patients is used to validate targets for drug action and to optimize clinical treatment.

An important prerequisite for drug development is that the molecule maintains its properties after labeling. This is a reason for the common use of the short-lived

positron-emitting radionuclide ^{11}C; the substitution of naturally occurring ^{12}C with ^{11}C does not change the biochemistry or the pharmacology of the molecule (Farde 1996).

At a PET measurement, a radiolabeled molecule (ligand) is injected intravenously and is distributed via the bloodstream to all parts of the body. The radioligand passes the blood-brain-barrier (BBB) and binds to target receptors as well as non-target proteins and extracellular matrix. When the radioactive atom in the molecule decays it emits a positron that collides with an electron one to a few millimeters away and annihilate. The annihilation produces two 511 keV gamma rays (i.e. two photons). The photons travel at approximately 180 degrees angle and are detected by a coincidence detector system outside the subject.

By using a complicated algorithm, an image of the regional radioactive decay can be calculated. In neuroreceptor imaging studies the regional radioactivity is corrected for decay and plotted versus time to yield time-activity curves or TACs. Different mathematical models are then applied on these TACs to calculate biological parameters describing ligand-receptor binding *in vivo*.

1.5 EARLY PET RADIOLIGANDS FOR PET IMAGING OF DOPAMINE D2 RECEPTORS

In the 1960s and 1970s the development of radioligand binding techniques and the availability of ^{3}H-labelled antipsychotic drugs with high specific radioactivity enabled a more direct study of dopamine receptors *in vitro* (Snyder 1978). With the development of the PET technology it became possible to study receptors in the living human brain. In 1983, pioneer work of Wagner and co-workers at John Hopkins university demonstrated binding of ^{11}C- N-metyl-spiperone ([^{11}C]NMSP) to dopamine D2 receptors in the human brain *in vivo* (Wagner et al. 1983). However, [^{11}C]NMSP and other spiperone derivates was shown to also have high affinity for $5HT_2$ and α_1 receptors (Leysen et al. 1978; Maziere et al. 1984; Wong et al. 1986). The salicylamid [^{11}C]raclopride was developed shortly thereafter (Farde et al. 1986). Its' affinity was lower than that of [^{11}C]NMSP but selective to the dopamine D2 and D3 receptor subtype. [^{11}C]raclopride and the spiperone derivates have been widely used in PET research on dopamine neurotransmission.

1.6 DYSFUNCTION OF THE DOPAMINE SYSTEM

Disturbed dopaminergic neurotransmission has been implicated in the patophysiology of several common and disabling neuropsychiatric disorders. In Parkinson's disease, the pathogenesis is directly linked to destruction or degradation of cells responsible for dopamine transmission. In other disorders, such as schizophrenia and ADHD, the role of the DA system remains to be clarified.

1.6.1 The dopamine hypothesis for schizophrenia

The present thesis represents development of methodology primarily intended for schizophrenia research. The dopamine hypothesis is accordingly presented in some detail.

Schizophrenia is a severe disabling psychiatric disorder with a lifetime risk of 0.8% (Carpenter and Buchanan 1994). The clinical manifestations are grouped into positive symptoms (i.e. mainly hallucinations and delusions), and negative symptoms (e.g blunted emotions). In addition to positive and negative symptoms, the disorder is accompanied by cognitive deficits, compulsions and affective symptoms.

The dopamine hypothesis of schizophrenia was developed during the 1960s and was based on several lines of research. First, it was shown that the antipsychotic effect of neuroleptic drugs was related to block of dopamine receptors (Carlsson and Lindqvist 1963; van Rossum 1966; Nyback and Sedvall 1970). Moreover, the clinical features of amphetamine, a drug that was known to increase dopamine transmission, resemble those of acute paranoid schizophrenia (Conell 1958). The dopamine hypothesis for schizophrenia was developed from the research on antipsychotic drugs and the observations with amphetamine. The hypothesis states that the symptoms of schizophrenia are due to overactivity of central dopamine transmission (Haracz 1982, review).

An initial PET study with [^{11}C]NMSP showed a two- to threefold increase in dopamine D2 receptor density in the striatum in drug naïve patients with schizophrenia when compared with normal controls (Wong et al. 1986). The finding of markedly increased receptor densities was, however, not supported in a study using [^{11}C]raclopride (Farde et al. 1987; Farde et al. 1990). A meta-analysis of sub sequential studies provides some support for a small elevation of D2 receptor density in the striatum in patients with schizophrenia (Laruelle 1998).

Later hypothesis has proposed differential hypo- and hyperactivity in different dopaminergic pathways (Weinberger 1987). According to this hypothesis, the positive symptoms of schizophrenia may correspond to hyperactivity in the nigro-striatal pathway whereas negative symptoms may correspond to hypoactivity in the meso-limbic pathways. Confirmation of this hypothesis requires a detailed analysis of dopaminergic neurotransmission throughout the entire brain.

The dopamine hypothesis has recently been supported by some interesting imaging studies measuring D2 receptor binding after small doses of amphetamine (Laruelle et al. 1996; Breier et al. 1997). Radioligand binding was more markedly reduced in patients with schizophrenia as compared with controls indicating a larger effect of amphetamine on dopamine release in patients with schizophrenia.

1.6.2 Extrastriatal dopamine regions in schizophrenia

Besides the striatum, several other regions have since long been implicated in the patophysiology of schizophrenia. The lack of suitable radioligands for regions with low receptor density has, however, hampered direct imaging studies in these regions. The extrastriatal regions of interests in schizophrenia research are among others the thalamus were post mortem studies indicate cell loss and decreased volume in the mediodorsal nucleus as well as the pulvinar (Pakkenberg 1992; Byne et al. 2002).

Besides the thalamus, several cortical regions are of interests; the frontal cortex partly due to inability of patients to increase blood flow during psychological tests sensitive to frontal lobe functioning (Weinberger et al. 1986), the temporal cortex due to the common auditory hallucinations in schizophrenia (Dierks et al. 1999; Lennox et al. 2000) and the anterior cingulate because its' involvement in motor control, cognition and arousal/drive state (Paus 2001). The cerebellum is also of high interest since it is a part of the cortico-cerebellar-thalamic-cortical circuit thought of as pivotal for smooth coordination of both motor and cognitive functioning and defective in schizophrenia (Andreasen et al. 1999).

The pituitary is not a site primarily involved in schizophrenia. However, antipsychotic drugs inhibit DA binding to receptors thereby causing an increase in serum prolactin levels. This effect is of clinical importance and explains the galactorrea and menstrual disturbances commonly recorded in women treated with antipsychotic drugs.

The D2 receptor density is low in these regions (Table 1-1). To measure such low receptor densities in regions of limited extent, a more sensitive methodology is needed than that used for the striatum, a large region with high density of receptors.

1.7 DOPAMINE D2 RECEPTOR OCCUPANCY

Receptor occupancy is a concept used to denote the percentage of a receptor population that is occupied by a drug. In imaging studies occupancy is usually estimated as the percentage reduction of specific binding following administration of a drug. High dopamine D2 receptor occupancy has consistently been demonstrated during treatment with classical antipsychotic drugs (Farde et al. 1986; Farde et al. 1988). In 1992, Farde and co-workers showed that a striatal dopamine D2 receptor occupancy of approximately 70-80% was clinically efficacious with low risk of extrapyramidal side-effects (EPS) (Farde et al. 1992).

Early PET measurements did not allow for determination of receptor occupancy in extrastriatal regions. A preferential dopamine D2 receptor blockade in extrastriatal regions of clozapine has more recently been reported using single photon emission tomography (SPET) and the high affinity radioligand [^{123}I]epidepride (Pilowsky et al. 1997). The finding has not been confirmed using PET and [^{11}C]raclopride to measure receptor occupancy in the striatum and [^{11}C]FLB 457 to measure occupancy in extrastriatal regions in the same subjects (Talvik et al. 2001).

1.8 STARTING POINT FOR THE THESIS

At the Karolinska Institutet, the new radioligand [^{11}C]FLB 457 was synthesized and examined by PET in the mid 1990s (Halldin et al. 1995; Farde et al. 1997). The radioligand has the very high affinity of 20 pM for dopamine D2 receptors *in vitro* (Hogberg 1993; Halldin et al. 1995) and allowed for visualization of extrastriatal dopamine receptors in the human brain *in vivo*. However, due to the very high affinity, the kinetic behavior was different from previously developed ligands for the dopamine system. The need for development of quantitative modeling of [^{11}C]FLB 457 binding was the starting point for the present thesis work.

2 AIMS

The overall objective of the thesis was to examine and compare methodologies for quantification of dopamine D2 receptor binding in extrastriatal regions in the human brain *in vivo* using PET and the new radioligand [^{11}C]FLB 457. More specifically the main objective can be divided into three parts, namely:

2.1 ON [^{11}C]FLB 457

- To examine the potential of the standard two-tissue compartment model and derived approaches for interpretation of time activity curves for [^{11}C]FLB 457 binding.
- To apply a cross validation approach and a simulation study in a comparison of potential and limitations of the quantitative approaches.
- To obtain absolute values of extrastriatal dopamine D2 receptor concentrations and affinity in the living human brain.

2.2 ON EXTRASTRIATAL RECEPTOR OCCUPANCY

- To examine the validity of commonly used ratio approaches for measurements of drug induced receptor occupancy when applied to the high affinity radioligand [^{11}C]FLB 457.
- To critically examine the use of an *in vivo* Scatchard procedure for analyzes of [^{11}C]FLB 457 binding.
- To critically examine the emerging concept of "receptor occupancy half-life", i.e. the time for receptor occupancy to decrease to half of its initial value after discontinuation of drug treatment.

2.3 ON THE PITUITARY

- To visualize and quantify dopamine D2 receptors in the normal human pituitary, a gland located outside the BBB.

3 SUBJECTS AND METHODS

3.1 SUBJECTS

In paper I, seven males and one female, age 23 to 38 years, participated in one PET-measurement. They were all healthy according to history, physical examination, psychiatric interview, blood and urine analysis and magnetic resonance imaging (MRI) of the brain. They did not use any medication and were all non-smokers. In paper III, the same subjects participated in one ore two additional PET-measurement with different specific radioactivities injected (see more below). In addition, in study III the number of subjects were increased by two female healthy subjects (37 and 22 years old) who participated in two PET-measurement with high and low mass of [^{11}C]FLB 457 injected, respectively. The two additional female subjects were healthy according to the above-mentioned criteria. In paper V, the same subjects as in paper I participated.

3.2 RADIOCHEMISTRY

Altogether ten subjects were examined with high and low specific radioactivity (SA) injected. In study I only high SA was injected whereas in study III and V both high and low SA was injected.

The specific radioactivity at the time of injection in study I varied between 1081 and 2086 Ci/mmol and the radioactivity injected was 189 to 299 MBq (5.1 and 8.1 mCi). This corresponds to an injected mass FLB 457 of 1.1 to 2.1 μg.

In paper III and V, to differentiate receptor density and affinity also high mass of FLB 457 was injected. In these studies, the specific radioactivity at the time of injection varied between 163 and 4835 Ci/mmol and the radioactivity injected was 189 to 329 MBq (5.1 and 8.9 mCi). This corresponds to an injected mass FLB 457 of 0.5 to 18 μg.

3.3 MRI AND PET SYSTEMS

MRI scans were performed on a 1.5-T Signa unit (General Electric, Milwaukee). A standard spin–echo sequence with a 256x256 matrix was used with a repetition time of 4 seconds. Echo times were 17 msec for proton-density-weighted images and 85 msec for T2-weighted images.

The PET system used was Siemens ECAT Exact HR, which was run in the 3D-mode (Wienhard et al. 1994). The in plane and axial resolutions was 3.8 mm and 4.0 mm, respectively, full width half maximum (FWHM). A Hanning filter with a cut-off frequency 0.5 of maximum was used, providing an in-plain resolution of 5.5 mm FWHM. Scatter correction was performed as described in the literature (Wienhard et al. 1994). Attenuation correction was done using transmission scan data obtained for each subject. The reconstructed volume was displayed as 47 sections with a center-to-center distance of 3.125 mm.

A head positioning system was used in both the PET and MRI measurements to allow the same head positioning in the two imaging modalities (Bergstrom et al. 1981).

3.4 PET EXAMINATION PROCEDURE

In each PET-measurement the subject was placed recumbent with his head in the PET-system. An arterial cannula was inserted in the left arteria radialis and another cannula was inserted into the right antecubital vein. A sterile physiological phosphate buffer (pH=7.4) solution containing [^{11}C]FLB 457 was injected as a bolus during 2 seconds into the right cubital vein. The cannula was then immediately flushed with 8 ml saline. After injection of radioactive ligand, arterial blood samples were drawn from the cannula in the left arm (see below, section 3.5).

Brain radioactivity was measured in a series of consecutive time frames for up to 63 minutes. The frame sequence consisted of three 1-min frames followed by four 3-min frames followed by eight 6-min frames.

3.5 ARTERIAL BLOOD SAMPLING

In paper I and V arterial blood samples were used. To obtain the arterial blood samples, an automated blood sampling system was used during the first 5 minutes of each PET measurement (Farde et al. 1989). Thereafter, arterial blood samples were taken manually at the midpoint of each frame until the end of the measurement.

3.6 DETERMINATION OF RADIOACTIVE METABOLITES IN PLASMA

The fractions of plasma radioactivity corresponding to unchanged [^{11}C]FLB 457 and metabolites were determined (Halldin et al. 1995). Arterial plasma samples (2ml) were drawn at 4, 10, 20, 30, 40, 50 and 60 minutes post injection and analyzed by gradient High Performance Liquid Chromatography (HPLC). Fractions that correlated with standards of FLB 457 and the corresponding radioactivity peaks were collected and counted in a well counter. The radioactivity in a certain fraction was expressed as a percentage of the total radioactivity (Halldin et al. 1995).

3.7 REGION OF INTEREST (ROI)

In paper I and III, regions of interest (ROIs) were delineated on the MR-images according to anatomical boundaries and transferred to the corresponding reconstructed PET images. ROIs were defined for the thalamus, the lateral temporal cortex, the anterior cinguli, the frontal cortex and the cerebellum. The ROIs were delineated for both the left and the right side. For the cerebellum the ROIs were drawn in three adjacent sections while the ROIs for the other regions were delineated in four to five adjacent sections.

In paper V, to avoid motion artifacts, the dynamic PET-image was realigned to the tenth time frame of the PET image using the public available software SPM2 (Frackowiak et al. 1997). Regions of interests were delineated on the PET-images with the guidance of the MR-image. The ROIs for pituitary were drawn in two adjacent sections.

Data were pooled, so that the average radioactivity concentration for the whole volume of interest was obtained. To obtain regional time-activity curves (TACs), regional

radioactivity was calculated for each frame, corrected for decay and plotted versus time. It is worth noting that decay correction allows for division of the radioactivity concentration of the TAC with SA at time zero to obtain time curves for radioligand concentration.

3.8 THEORY

The two-tissue compartment model has been commonly used to describe regional time activity curves (TACs) of several neuroreceptor radioligands (figure 3-1)(Mintun et al. 1984; Blomqvist 1991). From the model the following equations can be derived:

$$dC_N(t)/dt = f_1 C_P(t) K_1 - f_2 k_2 C_N(t) - f_2 k_{on}(B_{\max} - C_B(t)/SA) C_N(t) + k_{off} C_B(t) \quad (1)$$

$$dC_B(t)/dt = f_2 k_{on}(B_{\max} - C_B(t)/SA) C_N(t) - k_{off} C_B(t) \quad (2)$$

$$C_T(t) = C_N(t) + C_B(t) \quad (3)$$

where *Cp(t)* is the metabolite corrected plasma input function (nCi ml^{-1}). $C_N(t)$ and $C_B(t)$ is the radioactivity concentration (nCi ml^{-1}) in the compartment representing not specifically bound and specifically bound radioligand, respectively. $C_T(t)$ is the brain tissue radioactivity (nCi ml^{-1}). K_1 and k_2 are first order rate constants for in- and out flux over the blood brain barrier, respectively (min^{-1}). The constant k_{on} is the bimolecular association rate constant (ml pmol^{-1} min^{-1}), B_{max} the concentration of receptors (nM), SA the specific radioactivity of the radioligand (Ci mmol^{-1}) and k_{off} the unimolecular dissociation rate constant (min^{-1}). f_1 and f_2 are the fractions of the total radioligand concentration that represents truly free and unbound radioligand in plasma and C_N, respectively.

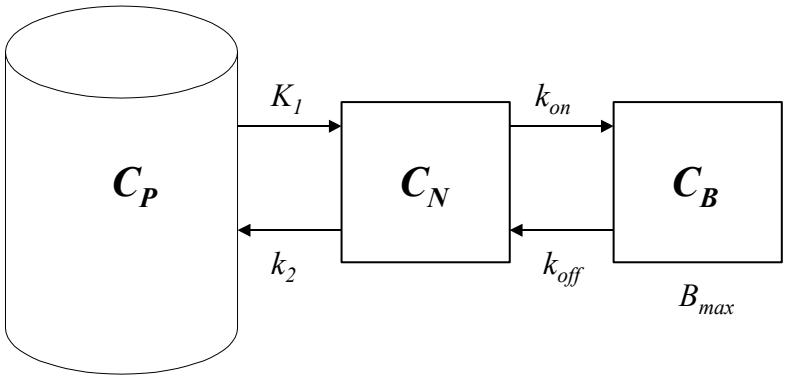

Figure 3-1. Standard two-tissue compartment model for radioligand uptake and binding in brain.

3.8.1 The concept of equilibrium

The theory for analysis of radioligand binding to receptors was initially developed for experiments in test tubes, allowing sufficient time for binding to reach equilibrium conditions. At equilibrium conditions it is possible to determine receptor density (B_{max}) and affinity (K_D) using simple non-differential equations. In experiments *in vivo* the radioligand is most often administered intravenously as a rapid bolus injection. After bolus injection there is an initial peak of the plasma radioactivity followed by a rapid fall that gradually gives way to a mono-exponential decline. The plasma input function will therefore change dramatically during PET data acquisition. Ideally, a kinetic analysis using a metabolite corrected plasma input function is then needed to obtain binding parameters that are valid for equilibrium conditions.

3.8.1.1 Peak equilibrium

To avoid cumbersome arterial blood sampling, the free and non-displaceable compartment $C_N(t)$ has been approximated with the time activity curve (TAC) from a reference tissue devoid of specific binding sites $C_{REF}(t)$ (Farde et al. 1986; Farde et al. 1989). The TAC for the specific binding has then been calculated as $C_T(t)$ minus $C_{REF}(t)$. However, the use of $C_{REF}(t)$ instead of $C_N(t)$ introduces a systematic error as has been demonstrated in later works (Farde et al. 1989; Lammertsma and Hume 1996; Ito et al. 1998). For [^{11}C]raclopride , $C_{REF}(t)$ and $C_N(t)$ are close and the error introduced when using $C_{REF}(t)$ instead of $C_N(t)$ is negligible.

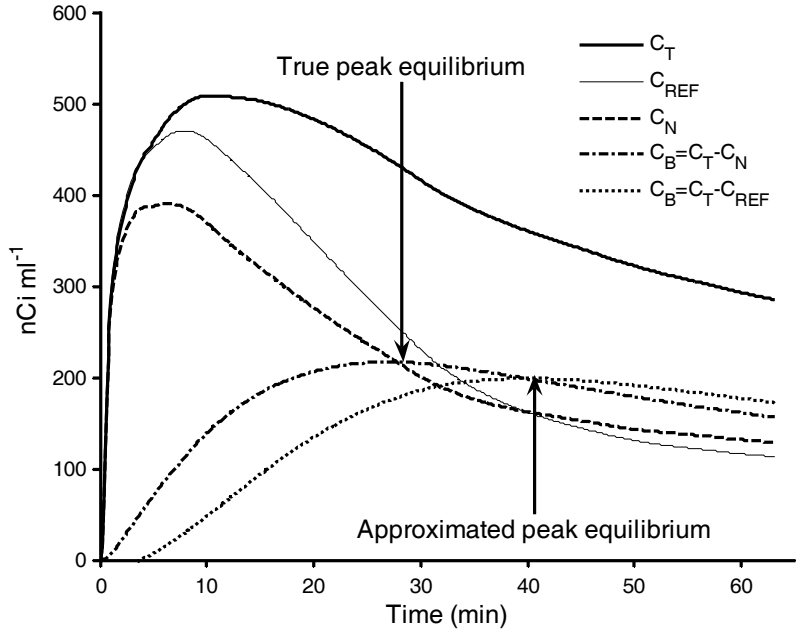

Figure 3-2. Simulated TACs after iv injection of [^{11}C]FLB 457. Solid lines represent TACs from an extrastriatal region (thick) and the cerebellum (thin). Dashed lines represent $C_N(t)$, $C_T(t)$-$C_{REF}(t)$ and $C_T(t)$-$C_N(t)$. The figure illustrates the difference in time between the approximated peak equilibrium and true peak equilibrium.

The moment when the TAC for the compartment representing specifically bound radioligand is at its' maximum is commonly denoted peak equilibrium and has been defined as occurring when $d(C_T(t)-C_{REF}(t))/dt=0$ (Farde et al. 1989). However, in this

thesis work, the moment when $d(C_T(t)-C_{REF}(t))/dt=0$ will be denoted "approximated peak equilibrium" and $d(C_T(t)-C_N(t))/dt=0$ will be defined as the "true peak equilibrium" (figure 3-2).

3.8.1.2 True equilibrium

The concept of true equilibrium requires that all derivates of the system are zero. Theoretically, peak equilibrium is not a true equilibrium of the entire system since only $dC_B(t)/dt$ but not $dC_N(t)/dt$ or $dC_P(t)/dt$ is zero at that moment. An *in vivo* approach to mimic the classical test tube analysis of receptor binding is to administer the radioligand as a continuous infusion. This paradigm will ideally produce true equilibrium, i.e. all derivates of the system will be zero. To achieve true equilibrium in reasonable time a bolus injection is often given before start of continuous radioligand infusion (Carson et al. 1993).

3.8.2 Regional radioligand occupancy

For commonly used radioligands with moderate affinity such as [^{11}C]raclopride, occupancy of the radioligand itself is of minor concern since only a small fraction of the total receptor population will be occupied. However, using extremely high affinity radioligands, such as [^{11}C]FLB 457, radioligand occupancy can be of concern since even very small masses of injected radioligand could produce significant receptor occupancy. In addition, in a bolus injection paradigm there may be regional differences in radioligand occupancy.

The following equations (equations 4-8) may serve as a basis for examination of radioligand occupancy. At true peak equilibrium and at true equilibrium equation 2 can be rewritten to:

$$\frac{B}{B_{\max}} = \frac{F}{(K_D + F)} \tag{4}$$

where F is the concentration of free and non-displaceable radioligand in tissue, i.e. $C_N(t)/SA$ (nM). $C_B(t)/SA$ equals B, the concentration of specifically bound radioligand (nM). K_D is the equilibrium dissociation constant and corresponds to the ratio k_{off}/k_{on} (nM). B/B_{max} is the ratio of bound radioligand to the total concentration of receptors, i.e. the occupancy produced by the radioligand itself. If SA is sufficiently high the ratio $C_N(t)/SA$ will be negligible. The concept of "tracer dose" is used to denote such high SAs. However, the definition of what is "negligible" has not been defined in the literature. Using tracer dose of injected radioligand equations 1 and 2 will revert to:

$$dC_N(t)/dt = f_1 C_P(t) K_1 - f_2 k_2 C_N(t) - f_2 k_3 C_N(t) + k_4 C_B(t) \tag{1a}$$

$$dC_B(t)/dt = f_2 k_3 C_N(t) - k_4 C_B(t) \tag{2a}$$

where k_3 (min^{-1}) is $k_{on}B_{max}$ and k_4 (min^{-1}) equals k_{off}. Using only tracer doses it is not possible to differentiate B_{max} and K_D (Mintun et al. 1984; Blomqvist 1991). Furthermore, at high SA, where $F << K_D$, equation 4 can be simplified to:

$$\frac{B}{F} \approx \frac{B_{\max}}{K_D} \tag{5}$$

where the ratio B_{max}/K_D corresponds to the binding potential (*BP*), a parameter that has extensively been applied as an index for receptor density (Mintun et al. 1984; Blomqvist 1991).

An expression for *F* can be derived by a combination of equations 1 and 2 and division by SA (Farde et al. 1989; Blomqvist 1991):

$$F = \frac{1}{SA}\left(\frac{K_1}{k_2}C_P(t) - \frac{1}{k_2}dC_T(t)/dt\right) \tag{6}$$

After insertion of equation 6 into equation 4, an expression is derived for the occupancy produced by the radioligand:

$$\frac{B}{B_{\max}} = \frac{\frac{1}{SA}\left(\frac{K_1}{k_2}C_P(t) - \frac{1}{k_2}dC_T(t)/dt\right)}{\left(K_D + \frac{1}{SA}\left(\frac{K_1}{k_2}C_P(t) - \frac{1}{k_2}dC_T(t)/dt\right)\right)} \tag{7}$$

This expression includes $dC_T(t)/dt$, $C_P(t)$, k_2 and the distribution volume (K_1/k_2) for $C_N(t)$.

Equation 7 highlights some important aspects of radioligand binding. $dC_N(t)/dt$ is less than zero at true peak equilibrium (Figure 3-2) (Carson et al. 1993). According to equation (3), the derivate $dC_T(t)/dt$ is less than zero since $dC_B(t)/dt=0$ at true peak equilibrium. This is of particular importance when doing regional comparisons among regions with different receptor densities thus having different $dC_T(t)/dt$. Given the same SA and the use of bolus injection, radioligand occupancy will be higher in ROIs with TACs that show steeper negative slope at true peak equilibrium, e.g. ROIs with low receptor densities.

Furthermore, based on the observation that true peak equilibrium appears earlier in low-density regions than in high-density regions, $C_P(t)$ at the early occurring true peak equilibrium in low-density regions can be predicted to be larger than $C_P(t)$ at the later occurring true peak equilibrium in high-density regions. The higher value of $C_P(t)$ combined with the more negative slope of $C_T(t)$ at true peak equilibrium in low density regions contribute to a larger *F* in low receptor density regions. According to equation 4, an increase in *F* will lead to an increase in occupancy. In conclusion, we would expect higher radioligand occupancy in regions with low as compared to high receptor density for any given SA after bolus injection of the radioligand.

A continuous infusion paradigm satisfies the conditions for true equilibrium, i.e. all derivates above including $dC_P(t)/dt$ are zero. If $dC_T(t)/dt$ is zero at true equilibrium equation 7 becomes:

$$\frac{B}{B_{\max}} = \frac{\frac{1}{SA}\left(\frac{K_1}{k_2}C_P(t)\right)}{\left(K_D + \frac{1}{SA}\left(\frac{K_1}{k_2}C_P(t)\right)\right)} \tag{8}$$

At true equilibrium receptor occupancy is thus only dependent on SA, K_1/k_2 and $C_P(t)$. Observe that radioligand occupancy will be the same in all ROIs irrespective of receptor density, since $C_P(t)$ is constant during true equilibrium conditions. Radioligand occupancy will thus not be dependant on $C_T(t)$ if a continuous infusion approach is used.

3.8.3 The Scatchard analysis

The Scatchard equation can be obtained by rearranging differential equation 2 (Scatchard 1949; Farde et al. 1989; Logan et al. 1997):

$$\frac{B}{F} = \frac{B_{\max} - B}{K_D} - \frac{1}{C_N(t)k_{off}}\frac{dC_B(t)}{dt} \tag{9}$$

At true peak equilibrium and true equilibrium, i.e when $dC_B/dt=0$, the second term on the right hand side is zero and the equation becomes the original *in vitro* Scatchard equation. When B/F is plotted versus B, the x-axis intercept is B_{max}, the y-axis intercept is BP ($=B_{max}/K_D$) and -1/slope is K_D. However, at approximated peak equilibrium $dC_B(t)/dt$ will not be zero and neither will the second term on the right hand side in equation 9.

Equation 9 provides the background for estimation of the error in the *in vivo* Scatchard plot when calculated by the use of the approximated peak equilibrium. For ligands like [^{11}C]raclopride and [^{11}C]cocaine the second term on the right hand side has been shown to be negligible and the method gives valid values for B_{max} and K_D (Farde et al. 1989; Logan et al. 1997).

3.9 CALCULATIONS AND SIMULATIONS

There are no analytical solutions for the above-mentioned standard two-tissue compartment model (equations 1-3), i.e. given the parameters K_1, k_2, k_{on}, k_{off} and B_{max} there is no equation describing the tissue time activity curve. Instead, the differential equations (equations 1 and 2) have to be solved numerically. However, the differential equations that describe measurements with tracer doses of radioligand injected (equations 1a and 2a) are linear and analytical solutions can be derived (Lammertsma et al. 1996). A standard strategy is to fit the measured time activity data to the model in a least squares sense.

Simulations are applied in paper II, III and IV this thesis work. Quantification of radioligand binding is based, in one way or another, on the two-tissue compartment model. Due to the fact that no simple analytical solutions can be found for this model, simulations are of value when one is trying to understand the temporal behavior of the system. It is important to know that simulations by themselves do not provide mathematical evidence. However, in empirical research, simulations serve as a tool when evaluating the explanatory and predictive powers of a given model.

In all papers, Matlab 6 to 6.5 was used in the calculations and simulations (The MathWorks Inc. ©).

3.10 SAMPLE SIZE

Eight to ten healthy subjects participated in this thesis (paper I and V and paper III, respectively). The subjects participated in twentysix PET-measurements altogether. The numbers of subjects and measurements are thus small. The need for development of methodology in quantification of [^{11}C]FLB 457 binding was the starting point for the present thesis (see section 1.8). The aim was thus not to describe group differences but to develop methods for applied clinical studies.

3.11 ETHICAL CONSIDERATIONS

The studies were approved by the Ethics and Radiation Safety committee of the Karolinska Hospital. All subjects were included after giving informed consent according to the Declaration of Helsinki.

Even though arterial puncture is performed with local anesthesia, it may cause some pain and discomfort and there is a potential for hemorrhage. Furthermore, the total radioactivity exposure is comparable to the background radiation an individual is exposed to living in Stockholm during one year. The helmet used in PET and MRI measurements may cause discomfort.

Exposure for radiation, pain, risk for hemorrhage and discomfort during PET and MRI measurements in ten subjects have to be balanced with the delivery of new methodologies for examination of the dopamine system in common and most often life-long disabling disorders, e.g. schizophrenia. My view is that the gains overrule the discomforts and risks. This view was confirmed by the participated subjects who did well tolerate the experimental procedure.

4 RESULTS AND COMMENTS

4.1 QUANTIFICATION OF [^{11}C]FLB 457 BINDING TO EXTRASTRIATAL DOPAMINE RECEPTORS IN THE HUMAN BRAIN (PAPER I)

This study in eight healthy subjects was designed to evaluate the suitability of the high affinity radioligand [^{11}C]FLB 457 for quantification of extrastriatal dopamine D2/D3 receptors in the human brain *in vivo*. [^{11}C]raclopride and [^{11}C]MNSP are the radioligands that have been most widely used for PET measurements of dopamine D2-like receptors (Wagner et al. 1983; Farde et al. 1989). However, a limitation with [^{11}C]raclopride is the comparatively low affinity for dopamine D2 receptors (1 to 2 nM) rendering it of little use in quantification of low receptor density regions (Farde et al. 1985), albeit attempts have been made to measure binding in the thalamus (Hirvonen et al. 2003; Kaasinen et al. 2004; Penttila et al. 2004). [^{11}C]MNSP, on the other hand, has higher affinity (0.1 to 0.3 nM) but also binds to $5HT_2$ and α_1 receptors (Lyon et al. 1986).

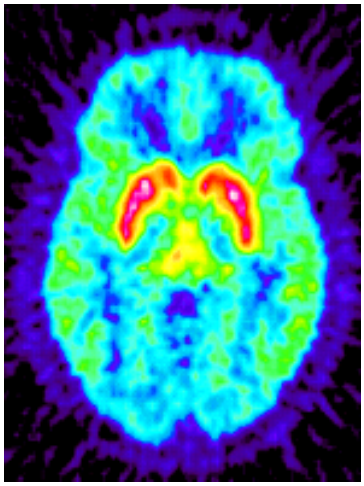

PET-measurements were acquired in the three-dimensional mode and arterial samples were drawn throughout the measurements and corrected for metabolites. The standard two-tissue compartment model and four derived approaches were applied to calculate and compare the binding potential (*BP*).

Figure 4-1. Summation image between 7.5 and 60 minutes showing regional radioactivity after iv injection of [^{11}C]FLB 457 in one healthy subject.

Besides the striatum, conspicuous radioactivity was accumulated in several extrastriatal regions such as the thalamus, the anterior cinguli, and the temporal and frontal cortices. The standard two-tissue compartment model could describe the measured time activity curves from the various regions of interest. The different derived approaches gave similar *BP* values and the rank order between regions was consistent with that found *in vitro*. The short acquisition time of only 63 minutes was not sufficient for reliable quantification of binding in the high receptor density regions of striatum.

This study shows that [^{11}C]FLB 457 can be used to visualize and quantify low dopamine D2 and D3 receptor density populations in the human brain *in vivo*. Furthermore, there was no strong support for specific binding in the cerebellum, indicating that simplified quantitative approaches that make use of cerebellum as reference tissue devoid of specific binding sites could be used in applied clinical studies.

4.2 POTENTIALS AND PITFALLS USING HIGH AFFINITY RADIOLIGANDS IN PET AND SPET DETERMINATIONS ON REGIONAL DRUG INDUCED D2 RECEPTOR OCCUPANCY – A SIMULATION STUDY BASED ON EXPERIMENTAL DATA (PAPER II)

Several quantitative approaches have been applied in PET studies throughout the years. The most simple approach is based on the observation that the ratio of radioactivity in a region with specific binding to that in a reference region devoid of specific binding approaches an asymptote during the late phase of data acquisition. This ratio has been referred to as secular equilibrium (Farde et al. 1989) or transient equilibrium (Carson et al. 1993) and has particularly often been used in applied single photon emission tomography (SPET) studies. Theoretically, a more appealing definition of equilibrium is when the derivate of the specific binding is zero, i.e., when the time activity curve for specific binding reaches a peak. Our initial observations with the high affinity radioligand [^{11}C]FLB 457 suggested that successful use of simple ratio analyses for previously established radioligands did not warrant use of the same approaches for high affinity radioligands.

The time of binding equilibrium is a critical variable for valid determination of receptor density and drug induced occupancy using [^{11}C]FLB 457 and simple ratio approaches. An early observation has been that the time of the equilibrium appears earlier when the density of available receptors is low.

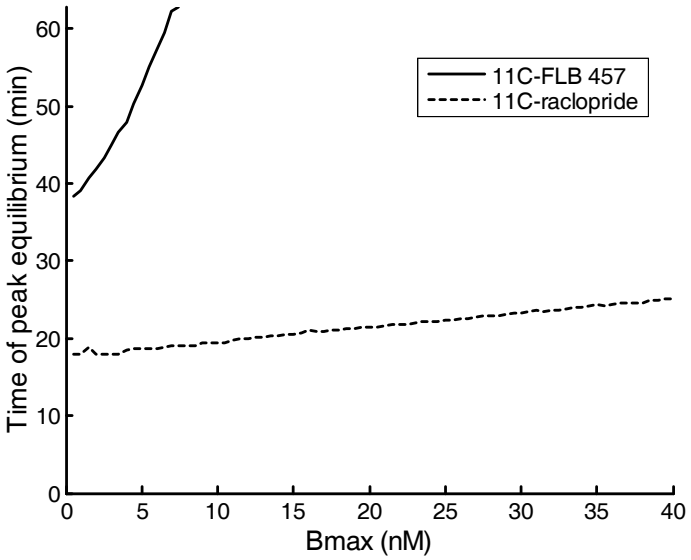

Figure 4-2. Simulated data showing time of peak equilibrium for [^{11}C]FLB 457 and [^{11}C]raclopride versus receptor density in the ROI.

The aim of this simulation study was to investigate the effect of receptor density on the time required to reach equilibrium for specific binding. In a second step we examined how errors produced by inaccurate determination of the binding parameter using simple ratio approaches propagate to the calculations of drug induced receptor occupancy. In a third step we used the commonly used simplified reference tissue model (SRTM) approach to calculate the drug induced receptor occupancy (Lammertsma and Hume 1996). Finally a comparison between the different approaches was made. Experimental data for [^{11}C]FLB 457 were used in a series of simulations and data for [^{11}C]raclopride were used as reference.

The simulations showed a marked effect of receptor density on equilibrium time for [^{11}C]FLB 457, but not for [^{11}C]raclopride (figure 4-2). For [^{11}C]FLB 457, a receptor density above about 7 nM caused the time of equilibrium to fall beyond time of data acquisition (i.e. 63 minutes). The use of preequilibrium data caused the ratio approaches but not the simplified reference tissue model (SRTM) approach to underestimate the binding potential and thus also the drug occupancy calculated for high-density regions. The study supports the use of ratio and SRTM analyses in extrastriatal low-density receptor regions for which the high affinity ligand [^{11}C]FLB 457 was developed. In high-density regions such as the human striatum simple ratio approaches cannot be validly applied, whereas the SRTM approach has higher potential to provide valid estimates.

4.3 DIFFERENTIATION OF EXTRASTRIATAL DOPAMINE D2 RECEPTOR DENSITY AND AFFINITY IN THE HUMAN BRAIN USING PET (PAPER III)

Most PET studies are based on only a single measurement after injection of a radioligand with high specific radioactivity. Such studies provide the binding potential (*BP*) (Mintun et al. 1984; Blomqvist 1991), i.e. the ratio of receptor density (B_{max}) and affinity (K_D). However, using a parameter like *BP* it is not possible to distinguish "B_{max}"-diseases that affects the receptor density, from "K_D "-diseases that affect the apparent affinity, e.g. the receptor protein structure or levels of endogenous dopamine. In many applied studies, the more easily obtained parameter *BP* has nevertheless been used as an index of receptor density.

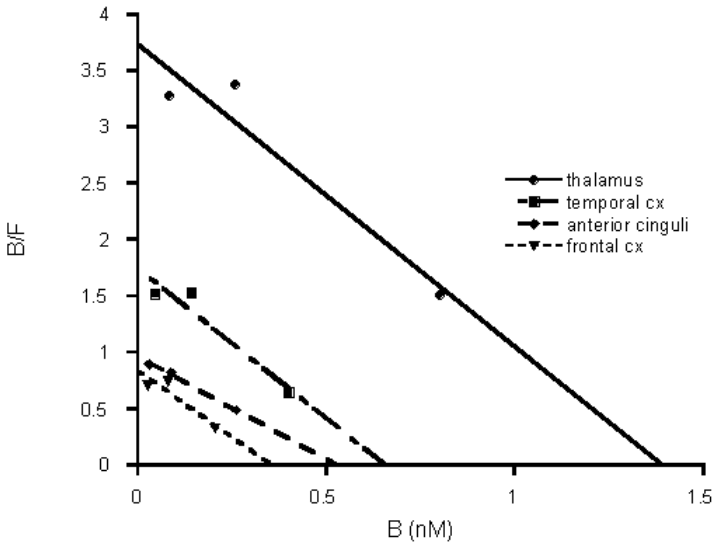

Figure 4-3. Three point saturation analysis in four different ROIs from one individual after iv injection of [^{11}C]FLB 457. The approximated peak equilibrium method was used to calculate B and B/F.

Differentiation of B_{max} from K_D requires a more demanding procedure with at least two PET measurements (Farde et al. 1986) or one measurement with multiple injections of radioligand (Delforge et al. 2001). In such procedures saturability of radioligand

binding to receptors is demonstrated by a series of PET measurements with different mass of radioligand. Binding parameters can then be determined either by kinetic compartmental analysis or by a linear analysis such as the Scatchard plot (Farde et al. 1986; Delforge et al. 2001).

The aim of this study was to determine absolute values for dopamine D2-like receptor density (B_{max}) and apparent affinity (K_D) in extrastriatal regions. Ten control subjects were examined according to a simple ratio saturation procedure including at least two PET measurements (Scatchard analysis). The procedure was critically examined using simulations based on parameters previously obtained from the two-tissue compartment model and a metabolite corrected arterial input function.

The calculated regional receptor density values were of the same magnitude (0.33 to 1.68 nM) and showed the same rank order as reported from post-mortem studies, i.e. in descending order thalamus, lateral temporal cortex, anterior cinguli and frontal cortex. The affinity ranged from 0.27 to 0.43 nM, i.e. approximately ten to twenty times the value found *in vitro* (20 pM). The area under the cerebellar time activity curve (TAC) was slightly lower (11±8%, mean±SD, p=0.004, n=10) after injection of low as compared with high specific radioactivity indicating sensitivity to the minute density of dopamine D2-like receptors in the this region.

ROI	B_{max} *in vivo* This study (*nM*)	B_{max} *in vivo* (Suhara et al. 1999) (*nM*)	B_{max} *in vitro* (Kessler et al. 1993) (*pmol/g tissue*)
Thalamus	1.68	2.3	0.72-1.0
Temporal cortex	0.60	1.5	0.28
Anterior cinguli	0.55	-	0.26
Frontal cortex	0.33	0.8	0.17

Table 4-1. Comparison of regional dopamine D2 receptor density values obtained in three different studies in the human brain.

The result of the present study support that dopamine D2 receptor density and affinity can be differentiated in low receptor density regions using a saturation approach. There was a significant ($p<0.001$) correlation between the binding potential calculated with SRTM and the receptor density (B_{max}), which supports the use of *BP* in clinical studies where differentiation of B_{max} and K_D is not required. In such studies the mass of FLB 457 has to be less than 0.5 μg injected to avoid a mass effect of the radioligand itself.

4.4 "RECEPTOR OCCUPANCY HALF-LIFE" – A MEANINGLESS CONCEPT (PAPER IV)

The concept of "receptor occupancy half-life" has been suggested to represent the time for receptor occupancy to reach half of its initial value. The concept has been used in

recent efforts to understand differences between time-courses of drug-receptor interaction in brain and drug concentration in plasma.

The concept of receptor occupancy half-life is, however, not defined by theory, as is the case with the half-life of a drug in plasma. This is because the time-course of drug–receptor interaction is described by a hyperbolic curve whereas the time-course for plasma drug concentration is described by a mono-exponential curve.

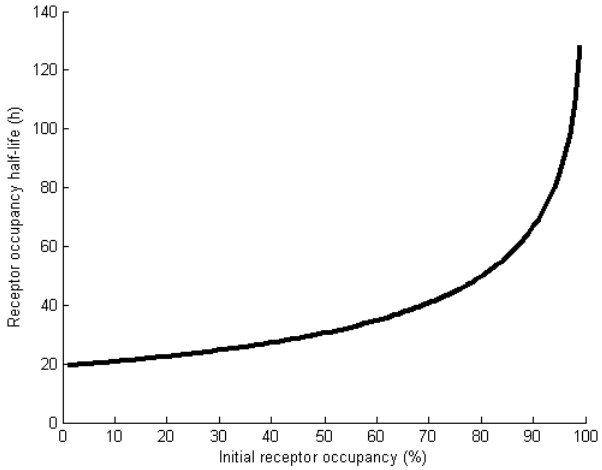

Figure 4-4. Simulated receptor occupancy half-life as a function of drug plasma concentration elimination constant (0.036 h^{-1}) and initial receptor occupancy. Note that receptor occupancy half-life is close to the half-life for drug concentration in plasma when initial receptor occupancy is small.

This work expresses concerns that the concept would run the risk of increasing the confusion rather than providing clarity. We, therefore, argue that the concept is meaningless and should be dropped altogether.

4.5 VISUALIZATION AND QUANTIFICATION OF DOPAMINE D2 RECEPTORS IN THE HUMAN PITUITARY USING PET AND [^{11}C]FLB 457 (PAPER V)

There is a marked difference in the ability of different antipsychotic drugs to elevate serum prolactin levels. The reasons for this are not completely understood. Importantly, the anterior pituitary gland, the location of the prolactin-secreting cells, is located outside the blood-brain-barrier (BBB), whereas the clinical effect of antipsychotic drugs is mediated through dopamine D2 receptors behind the BBB. It has been suggested that the concentration ratio of drug in plasma and brain vary among different antipsychotic drugs and may correspond to differential receptor occupancies behind and outside BBB, respectively. Such differences in receptor occupancy at target receptor populations could explain the differences in serum prolactin elevation observed with different antipsychotic drugs in clinical doses.

The hypothesis of differences in dopamine D2 receptor occupancy between brain and pituitary has received experimental support by a recent study in rodents *ex vivo* (Kapur et al. 2002). However, the observation has not been confirmed *in vivo* in the human brain due to lack of suitable radioligands for positron emission tomography (PET) or single photon emission tomography (SPET) imaging of dopamine D2 receptor binding in the pituitary.

The aim of this study in eight healthy subjects was to visualize dopamine D2 receptors in the human anterior pituitary gland *in vivo* using PET and [^{11}C]FLB 457. A second aim was to examine the potential of [^{11}C]FLB 457 for differentiation of dopamine D2 receptor density (B_{max}) and affinity (K_D) by using a kinetic saturation approach with metabolite corrected plasma concentration of radioligand as input function. To validate the use of more simple approaches, the binding potential (*BP*) obtained by a linear graphical analysis (Logan et al. 1996) was compared with the obtained B_{max}.

After injection of [^{11}C]FLB 457 with high SA there was a conspicuous accumulation of radioactivity in the pituitary (Figure 4-5). The magnitude and shape of the TACs obtained in the pituitary were comparable with the TACs of regions behind BBB known to express dopamine D2 receptors, e.g. the thalamus. In all subjects the TACs were lower after injection of a high mass of FLB 457, i.e. with low SA. There was a significant reduction of area under the TAC (AUC) after injection of low SA as compared with high SA (n=8,p=0.0036,df=7).

Both measurements with high and low SA were used to calculate dopamine D2 receptor density (B_{max}) and affinity (K_D) in the pituitary. The model fit converged for all ROIs. The receptor density and affinity was calculated to 1.3±0.1 nM and 0.6±0.5 nM, respectively (mean and std, n=8). No significant correlation between B_{max} and K_D was shown (n=8, r=-0.0047, p=0.99).

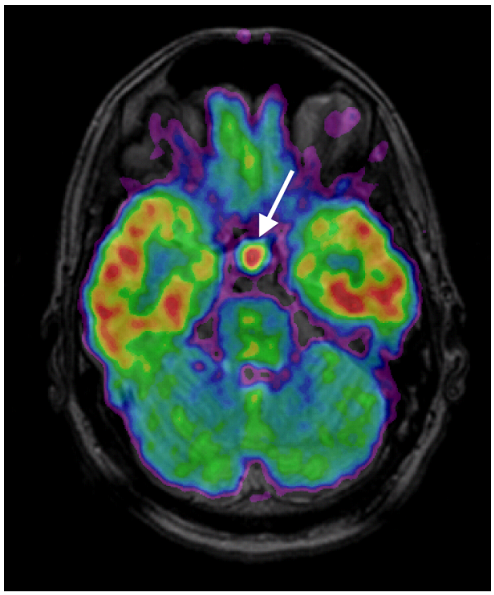

Figur 4-5. Summation image between 7.5 and 60 minutes showing regional radioactivity after iv injection of [^{11}C]FLB 457 in one healthy subject. The PET image is overlaid the corresponding MR-image. The arrow indicates the pituitary.

To investigate if the binding potential (*BP*) from a reference tissue approach would correlate with B_{max}, a linear graphical analysis was applied on the data from measurements with high SA. A linear phase was seen in all subjects after 18 minutes and, consequently, a linear fit was applied on the data obtained between 18 and 63 minutes. There was a significant correlation between B_{max} and *BP* (p=0.0058, n=8, df=7).

This work suggests that [^{11}C]FLB 457 can bee used to visualize dopamine D2 receptors in the healthy human pituitary *in vivo*. The binding show specificity due to its' saturability with high mass of FLB 457 injected. Receptor density and affinity can be

differentiated and quantified using standard kinetic procedures and the *BP* obtained with the linear graphical analysis correlates with B_{max} indicating that this approach can be used in clinical applied studies.

5 SUMMARY OF FINDINGS

5.1 ON [^{11}C]FLB 457

- [^{11}C]FLB 457 binding to extrastriatal regions could be described by the two-tissue compartment model and the rank order of regional binding potential (*BP*) values was consistent with the rank order reported in binding studies on human brain tissue postmortem.
- The binding potential (*BP*) obtained for the striatum, i.e. the region with highest density, was underestimated since ^{11}C-labeled FLB457 only allows for an acquisition time of about 1 hour.
- The regional receptor density (B_{max}) values obtained by Scatchard analysis were close to the *in vitro* values given in the literature.
- The affinity was about 10 to 20 times lower *in vivo* indicating that the free radioligand concentration in the extracellular space represents only a minor fraction of non-displaceable radioligand in brain.
- With regard to the cerebellum as reference region for non-displaceable binding it can not be excluded that [^{11}C]FLB 457 is sensitive to the minute receptor density of dopamine D2 receptors in this region.

5.2 ON EXTRASTRIATAL RECEPTOR OCCUPANCY

- Experimental data and simulation studies showed that the time to reach peak of specific radioligand binding is dependent on regional receptor density and varied between 39 and 63 minutes due to the several-fold difference in dopamine D2 receptor density across brain regions.
- Ratio methods underestimate drug-induced occupancy particularly in regions with high receptor density whereas the Simplified Reference Tissue Model (SRTM) yielded valid estimations.
- Theoretical considerations illustrated by a simulation approach showed that the emerging concept of "receptor occupancy half-life" is not supported by theory. Instead, initial receptor occupancy and the time-constant for drug clearance in plasma can be used in clinical studies to estimate the net-dissociation of a drug from the receptors.
- Simulations showed that the mass of FLB 457 injected has to be less than 0.5 µg to avoid a mass effect of the radioligand itself.

5.3 ON THE PITUITARY

- [^{11}C]FLB 457 can be used to visualize and quantify binding in the non-diseased human pituitary. The calculated receptor density is consistent with *in vitro* values.

6 FUTURE RESEARCH

6.1 THE PITUTARY

[^{11}C]FLB 457 and PET are tools for visualization and quantification of dopamine D2 receptors in the non-diseased human pituitary. In study V in this thesis, the only female who participated showed the highest receptor density (B_{max}) of all subjects. The study was not optimized for visualization and quantification of dopamine D2 receptors in the pituitary since it was an extended analysis of earlier work and the sample was small. To investigate gender differences in dopamine D2 receptor density in the human pituitary, a larger sample of both men and women is needed.

As mentioned in paper V, there is a marked difference in the ability of different antipsychotic drugs to elevate serum prolactin levels when used in clinical dosing. The hypothesis of a different concentration ratio of drug in plasma and brain among different antipsychotic drugs corresponding to differential receptor occupancies behind and outside BBB can now be tested by direct measurements with [^{11}C]FLB 457 on drug induced receptor occupancy in the pituitary. In a first step, to avoid cumbersome arterial blood sampling, the simple linear graphical analysis can be applied since the *BP* obtained with this method correlates with B_{max}.

6.2 STATISTICAL PARAMETRIC MAPPING (SPM)

Statistical Parametric Mapping (SPM) refers to the construction and assessment of spatially extended statistical processes used to test hypotheses about functional imaging data. To use SPM in receptor studies, a first step is to generate a parametric image, i.e. a three-dimensional image where each voxel represents a calculated parameter, such as receptor density (B_{max}) (Blomqvist et al. 1990). The parametric images can in sub sequential steps be used in group-comparisons and in statistical tests using the public available SPM software.

Co-workers at the Karolinska Institutet have developed a sophisticated algorithm that can be used to cluster TACs in order to reduce noise (Cselényi et al. 2005). The denoised TACs can in sub sequential analyses be used to calculate the sought for binding parameter on a voxel basis. A future objective is thus to use this algorithm and the standard non-linear two-tissue compartment model to generate parametric images of dopamine D2 receptor density (B_{max}) and affinity (K_D).

7 ACKNOWLEDGEMENTS

This thesis work is based on collaborations of many individuals to whom I want to express my sincere gratitude. Without you this work would never have been done.

Professor Lars Farde, my tutor, for introducing me to the fascinating world of neuroscience and receptors, for teaching the art of research and scientific writing, for enduring encouragements when times were tough and for his friendship.

Professor Christer Halldin, for making [^{11}C]FLB 457 available to us, for his expert knowledge in the field of radiochemistry, for co-authorship and close collaboration with professor Lars Farde.

Associate professor Carl Gunnar Swhan, for determination of metabolites, co-authorship and scientific discussions.

Research nurse Kjerstin Lind-Lindquist, for her excellent technical assistance during the PET measurements and otherwise, for her enjoyable friendship.

Associate professor Balász Guluyás, for his untamed enthusiasm and solid knowledge in the field of neuroscience and for bringing so many competent Hungarians to work with us.

Dr Zolt Cselényi, one of the able Hungarians, for the fruitful intellectual discussions and mind storms in the "Hungarian room", for appreciating the high mountains of Debrecen and for his friendship. Igen!

Dr Per Karlsson, for helping me with the first basic steps in the technology of PET research and for still helping me with admirable patience.

Dr Stefan Pauli, for enthusiasm, friendship and an ever-associating mind.

Drs Bengt Andrée and Mirjam Talvik, two of my brothers and sisters in arms, for long discussions, enjoyable travels and for catching the plane in Milano.

Drs Johan Lundberg, Judit Sóvágó and Nina Erixon, for their warm company, enthusiasm and friendship in the line outside Lars' door.

All new and old research colleagues and friends in the Karolinska PET group.

All members in the radiochemistry group, also including former members, such as Drs Camilla Lundquist and Johan Sandell, for radiochemical synthesis and great flexibility.

Associate professor Anna-Lena Nordström and Dr Svante Nyberg, co-authors and senior psychiatrists, for clinical guidance and for stressing the importance of evidence based psychiatry.

Ulla-Kajsa Persson, for exceptional secretarial work.

All our friends and relatives for just being there. You know who you are!

Marit and Bengt Olsson, my parents, and Birgitta and Tage Johansson, my parents in-law, for helping us with the kids and always giving us support, hope and strength to realize this project.

Kristina, my wife, life-companion and beloved, for her support, patience and sacrifice throughout the years. Thank you and forgive me for the hours, days, and weeks I have been absent from home. Without you, this thesis could not have been done at all.

Gustav, Johan and Klara, my kids, who had to put up with my work and absence when I really should have spent the time with them.

Swedish Science Research Council, National Institute of Mental Health, Karolinska Institutet and Jönköping County Hospital for financial support.

7.1 ADDENDUM

Birgitta passed away after a short time of illness during the completion of this thesis work. Birgitta helped us with everlasting kindness and always with a positive mind. Her faith in God was strong enough to move mountains and even though her sight was dim she now sees face to face. We all miss her.

So teach us to number our days,
that we may gain a heart of wisdom.
Ps 90:12

8 REFERENCES

Andreasen, N. C., P. Nopoulos, D. S. O'Leary, D. D. Miller, T. Wassink, and M. Flaum. 1999. Defining the phenotype of schizophrenia: cognitive dysmetria and its neural mechanisms. *Biol Psychiatry* 46 (7):908-20.

Bergstrom, M., J. Boethius, L. Eriksson, T. Greitz, T. Ribbe, and L. Widen. 1981. Head fixation device for reproducible position alignment in transmission CT and positron emission tomography. *J Comput Assist Tomogr* 5 (1):136-41.

Blomqvist, G. 1991. Kinetic analysis. *Wien Klin Wochenschr* 103 (15):451-7.

Blomqvist, G., S. Pauli, L. Farde, L. Eriksson, A. Persson, and C. Halldin. 1990. Maps of receptor binding parameters in the human brain--a kinetic analysis of PET measurements. *Eur J Nucl Med* 16 (4-6):257-65.

Breier, A., T. P. Su, R. Saunders, R. E. Carson, B. S. Kolachana, A. de Bartolomeis, D. R. Weinberger, N. Weisenfeld, A. K. Malhotra, W. C. Eckelman, and D. Pickar. 1997. Schizophrenia is associated with elevated amphetamine-induced synaptic dopamine concentrations: evidence from a novel positron emission tomography method. *Proc Natl Acad Sci U S A* 94 (6):2569-74.

Byne, W., M. S. Buchsbaum, L. A. Mattiace, E. A. Hazlett, E. Kemether, S. L. Elhakem, D. P. Purohit, V. Haroutunian, and L. Jones. 2002. Postmortem assessment of thalamic nuclear volumes in subjects with schizophrenia. *Am J Psychiatry* 159 (1):59-65.

Carlsson, A., and M. Lindqvist. 1963. Effect of Chlorpromazine or Haloperidol on Formation of 3methoxytyramine and Normetanephrine in Mouse Brain. *Acta Pharmacol Toxicol (Copenh)* 20:140-4.

Carpenter, W. T., Jr., and R. W. Buchanan. 1994. Schizophrenia. *N Engl J Med* 330 (10):681-90.

Carson, R. E., M. A. Channing, R. G. Blasberg, B. B. Dunn, R. M. Cohen, K. C. Rice, and P. Herscovitch. 1993. Comparison of bolus and infusion methods for receptor quantitation: application to [18F]cyclofoxy and positron emission tomography. *J Cereb Blood Flow Metab* 13 (1):24-42.

Conell, P.H. 1958. *Amphetamine psychosis*, *Maudsley Monograph, No 5*: Chapman & Hall.

Cselényi, Z., H. Olsson, C. Halldin, B. Gulyás, and L. Farde. 2005. Mapping of binding parameters in the human brain using an artificial neural network approach to reduce the noise effect.

Delforge, J., M. Bottlaender, S. Pappata, C. Loc'h, and A. Syrota. 2001. Absolute quantification by positron emission tomography of the endogenous ligand. *J Cereb Blood Flow Metab* 21 (5):613-30.

Dierks, T., D. E. Linden, M. Jandl, E. Formisano, R. Goebel, H. Lanfermann, and W. Singer. 1999. Activation of Heschl's gyrus during auditory hallucinations. *Neuron* 22 (3):615-21.

Farde, L. 1996. The advantage of using positron emission tomography in drug research. *Trends Neurosci* 19 (6):211-4.

Farde, L., E. Ehrin, L. Eriksson, T. Greitz, H. Hall, C. G. Hedstrom, J. E. Litton, and G. Sedvall. 1985. Substituted benzamides as ligands for visualization of dopamine receptor binding in the human brain by positron emission tomography. *Proc Natl Acad Sci U S A* 82 (11):3863-7.

Farde, L., L. Eriksson, G. Blomquist, and C. Halldin. 1989. Kinetic analysis of central [11C]raclopride binding to D2-dopamine receptors studied by PET--a comparison to the equilibrium analysis. *J Cereb Blood Flow Metab* 9 (5):696-708.

Farde, L., H. Hall, E. Ehrin, and G. Sedvall. 1986. Quantitative analysis of D2 dopamine receptor binding in the living human brain by PET. *Science* 231 (4735):258-61.

Farde, L., A. L. Nordstrom, F. A. Wiesel, S. Pauli, C. Halldin, and G. Sedvall. 1992. Positron emission tomographic analysis of central D1 and D2 dopamine

receptor occupancy in patients treated with classical neuroleptics and clozapine. Relation to extrapyramidal side effects. *Arch Gen Psychiatry* 49 (7):538-44.
Farde, L., T. Suhara, S. Nyberg, P. Karlsson, Y. Nakashima, J. Hietala, and C. Halldin. 1997. A PET-study of [11C]FLB 457 binding to extrastriatal D2-dopamine receptors in healthy subjects and antipsychotic drug-treated patients. *Psychopharmacology (Berl)* 133 (4):396-404.
Farde, L., F. A. Wiesel, H. Hall, C. Halldin, S. Stone-Elander, and G. Sedvall. 1987. No D2 receptor increase in PET study of schizophrenia. *Arch Gen Psychiatry* 44 (7):671-2.
Farde, L., F. A. Wiesel, C. Halldin, and G. Sedvall. 1988. Central D2-dopamine receptor occupancy in schizophrenic patients treated with antipsychotic drugs. *Arch Gen Psychiatry* 45 (1):71-6.
Farde, L., F. A. Wiesel, S. Stone-Elander, C. Halldin, A. L. Nordstrom, H. Hall, and G. Sedvall. 1990. D2 dopamine receptors in neuroleptic-naive schizophrenic patients. A positron emission tomography study with [11C]raclopride. *Arch Gen Psychiatry* 47 (3):213-9.
Finnema, S, N Seneca, L. Farde, E Shchukin, J Sóvágó, B Gulyás, H Wikstrom, R. B. Innis, J Neumeyer, and C. Halldin. 2005. A preliminary PET evaluation of the new dopamine D2 receptor agonist 3 [11C]MNPA in Cynomolgus monkey. *Nuclear Medicine and Biology* in press (in press):in press.
Frackowiak, R., K. Friston, C. Frith, R. Dolan, and J. editors Mazziotta. 1997. *Human Brain Function*: Academic Press, USA.
Ganong, WF. 2003. *Review of Medical Physiology*. 21 ed: Lange Medical Books/McGraw-Hill Medical Publishing Division.
Gurevich, E. V., and J. N. Joyce. 1999. Distribution of dopamine D3 receptor expressing neurons in the human forebrain: comparison with D2 receptor expressing neurons. *Neuropsychopharmacology* 20 (1):60-80.
Hall, H., L. Farde, C. Halldin, Y. L. Hurd, S. Pauli, and G. Sedvall. 1996. Autoradiographic localization of extrastriatal D2-dopamine receptors in the human brain using [125I]epidepride. *Synapse* 23 (2):115-23.
Halldin, C., L. Farde, T. Hogberg, N. Mohell, H. Hall, T. Suhara, P. Karlsson, Y. Nakashima, and C. G. Swahn. 1995. Carbon-11-FLB 457: a radioligand for extrastriatal D2 dopamine receptors. *J Nucl Med* 36 (7):1275-81.
Haracz, J. L. 1982. The dopamine hypothesis: an overview of studies with schizophrenic patients. *Schizophr Bull* 8 (3):438-69.
Hirvonen, J., S. Aalto, V. Lumme, K. Nagren, J. Kajander, H. Vilkman, N. Hagelberg, V. Oikonen, and J. Hietala. 2003. Measurement of striatal and thalamic dopamine D2 receptor binding with 11C-raclopride. *Nucl Med Commun* 24 (12):1207-14.
Hogberg, T. 1993. The development of dopamine D2-receptor selective antagonists. *Drug Des Discov* 9 (3-4):333-50.
Hurd, Y. L., M. Suzuki, and G. C. Sedvall. 2001. D1 and D2 dopamine receptor mRNA expression in whole hemisphere sections of the human brain. *J Chem Neuroanat* 22 (1-2):127-37.
Ito, H., J. Hietala, G. Blomqvist, C. Halldin, and L. Farde. 1998. Comparison of the transient equilibrium and continuous infusion method for quantitative PET analysis of [11C]raclopride binding. *J Cereb Blood Flow Metab* 18 (9):941-50.
Kaasinen, V., S. Aalto, K. Nagren, and J. O. Rinne. 2004. Dopaminergic effects of caffeine in the human striatum and thalamus. *Neuroreport* 15 (2):281-5.
Kapur, S., X. Langlois, P. Vinken, A. A. Megens, R. De Coster, and J. S. Andrews. 2002. The differential effects of atypical antipsychotics on prolactin elevation are explained by their differential blood-brain disposition: a pharmacological analysis in rats. *J Pharmacol Exp Ther* 302 (3):1129-34.
Kessler, R. M., W. O. Whetsell, M. S. Ansari, J. R. Votaw, T. de Paulis, J. A. Clanton, D. E. Schmidt, N. S. Mason, and R. G. Manning. 1993. Identification of extrastriatal dopamine D2 receptors in post mortem human brain with [125I]epidepride. *Brain Res* 609 (1-2):237-43.
Lammertsma, A. A., C. J. Bench, S. P. Hume, S. Osman, K. Gunn, D. J. Brooks, and R. S. Frackowiak. 1996. Comparison of methods for analysis of clinical [11C]raclopride studies. *J Cereb Blood Flow Metab* 16 (1):42-52.

Lammertsma, A. A., and S. P. Hume. 1996. Simplified reference tissue model for PET receptor studies. *Neuroimage* 4 (3 Pt 1):153-8.
Laruelle, M. 1998. Imaging dopamine transmission in schizophrenia. A review and meta-analysis. *Q J Nucl Med* 42 (3):211-21.
Laruelle, M., A. Abi-Dargham, C. H. van Dyck, R. Gil, C. D. D'Souza, J. Erdos, E. McCance, W. Rosenblatt, C. Fingado, S. S. Zoghbi, R. M. Baldwin, J. P. Seibyl, J. H. Krystal, D. S. Charney, and R. B. Innis. 1996. Single photon emission computerized tomography imaging of amphetamine-induced dopamine release in drug-free schizophrenic subjects. *Proc Natl Acad Sci U S A* 93 (17):9235-40.
Lefkowitz, R. J., S. Cotecchia, P. Samama, and T. Costa. 1993. Constitutive activity of receptors coupled to guanine nucleotide regulatory proteins. *Trends Pharmacol Sci* 14 (8):303-7.
Lennox, B. R., S. B. Park, I. Medley, P. G. Morris, and P. B. Jones. 2000. The functional anatomy of auditory hallucinations in schizophrenia. *Psychiatry Res* 100 (1):13-20.
Leysen, J. E., C. J. Niemegeers, J. P. Tollenaere, and P. M. Laduron. 1978. Serotonergic component of neuroleptic receptors. *Nature* 272 (5649):168-71.
Logan, J., J. S. Fowler, N. D. Volkow, G. J. Wang, Y. S. Ding, and D. L. Alexoff. 1996. Distribution volume ratios without blood sampling from graphical analysis of PET data. *J Cereb Blood Flow Metab* 16 (5):834-40.
Logan, J., N. D. Volkow, J. S. Fowler, G. J. Wang, M. W. Fischman, R. W. Foltin, N. N. Abumrad, S. Vitkun, S. J. Gatley, N. Pappas, R. Hitzemann, and C. E. Shea. 1997. Concentration and occupancy of dopamine transporters in cocaine abusers with [11C]cocaine and PET. *Synapse* 27 (4):347-56.
Lyon, R. A., M. Titeler, J. J. Frost, P. J. Whitehouse, D. F. Wong, H. N. Wagner, Jr., R. F. Dannals, J. M. Links, and M. J. Kuhar. 1986. 3H-3-N-methylspiperone labels D2 dopamine receptors in basal ganglia and S2 serotonin receptors in cerebral cortex. *J Neurosci* 6 (10):2941-9.
Malmberg, A., D. M. Jackson, A. Eriksson, and N. Mohell. 1993. Unique binding characteristics of antipsychotic agents interacting with human dopamine D2A, D2B, and D3 receptors. *Mol Pharmacol* 43 (5):749-54.
Maziere, B., C. Loc'h, P. Hantraye, R. Guillon, N. Duquesnoy, F. Soussaline, R. Naquet, D. Comar, and M. Maziere. 1984. 76Br-bromospiroperidol: a new tool for quantitative in-vivo imaging of neuroleptic receptors. *Life Sci* 35 (13):1349-56.
Meador-Woodruff, J. H., V. Haroutunian, P. Powchik, M. Davidson, K. L. Davis, and S. J. Watson. 1997. Dopamine receptor transcript expression in striatum and prefrontal and occipital cortex. Focal abnormalities in orbitofrontal cortex in schizophrenia. *Arch Gen Psychiatry* 54 (12):1089-95.
Mintun, M. A., M. E. Raichle, M. R. Kilbourn, G. F. Wooten, and M. J. Welch. 1984. A quantitative model for the in vivo assessment of drug binding sites with positron emission tomography. *Ann Neurol* 15 (3):217-27.
Missale, C., S. R. Nash, S. W. Robinson, M. Jaber, and M. G. Caron. 1998. Dopamine receptors: from structure to function. *Physiol Rev* 78 (1):189-225.
Narendran, R., D. R. Hwang, M. Slifstein, P. S. Talbot, D. Erritzoe, Y. Huang, T. B. Cooper, D. Martinez, L. S. Kegeles, A. Abi-Dargham, and M. Laruelle. 2004. In vivo vulnerability to competition by endogenous dopamine: comparison of the D2 receptor agonist radiotracer (-)-N-[11C]propyl-norapomorphine ([11C]NPA) with the D2 receptor antagonist radiotracer [11C]-raclopride. *Synapse* 52 (3):188-208.
Nyback, H., and G. Sedvall. 1970. Further studies on the accumulation and disappearance of catecholamines formed from tyrosine-14C in mouse brain. Effect of some phenothiazine analogues. *Eur J Pharmacol* 10 (2):193-205.
Pakkenberg, B. 1992. The volume of the mediodorsal thalamic nucleus in treated and untreated schizophrenics. *Schizophr Res* 7 (2):95-100.
Paus, T. 2001. Primate anterior cingulate cortex: where motor control, drive and cognition interface. *Nat Rev Neurosci* 2 (6):417-24.
Penttila, J., J. Kajander, S. Aalto, J. Hirvonen, K. Nagren, T. Ilonen, E. Syvalahti, and J. Hietala. 2004. Effects of fluoxetine on dopamine D2 receptors in the human

brain: a positron emission tomography study with [11C]raclopride. *Int J Neuropsychopharmacol* 7 (4):431-9.
Pilowsky, L. S., R. S. Mulligan, P. D. Acton, P. J. Ell, D. C. Costa, and R. W. Kerwin. 1997. Limbic selectivity of clozapine. *Lancet* 350 (9076):490-1.
Rieck, R. W., M. S. Ansari, W. O. Whetsell, Jr., A. Y. Deutch, and R. M. Kessler. 2004. Distribution of dopamine D2-like receptors in the human thalamus: autoradiographic and PET studies. *Neuropsychopharmacology* 29 (2):362-72.
Scatchard, G. 1949. The attraction of proteins for small molecules and ions. *Ann N Y Acad Sci* 51:660-672.
Snyder, S. 1978. *Overview of neurotransmittor receptor binding*. Edited by H. Yamamura, *Neurotransmitter receptor binding*: Raven Press.
Suhara, T., Y. Sudo, T. Okauchi, J. Maeda, K. Kawabe, K. Suzuki, Y. Okubo, Y. Nakashima, H. Ito, S. Tanada, C. Halldin, and L. Farde. 1999. Extrastriatal dopamine D2 receptor density and affinity in the human brain measured by 3D PET. *Int J Neuropsychopharmcol* 2 (2):73-82.
Talvik, M., A. L. Nordstrom, S. Nyberg, H. Olsson, C. Halldin, and L. Farde. 2001. No support for regional selectivity in clozapine-treated patients: a PET study with [(11)C]raclopride and [(11)C]FLB 457. *Am J Psychiatry* 158 (6):926-30.
Wagner, H. N., Jr., H. D. Burns, R. F. Dannals, D. F. Wong, B. Langstrom, T. Duelfer, J. J. Frost, H. T. Ravert, J. M. Links, S. B. Rosenbloom, S. E. Lukas, A. V. Kramer, and M. J. Kuhar. 1983. Imaging dopamine receptors in the human brain by positron tomography. *Science* 221 (4617):1264-6.
Vallone, D., R. Picetti, and E. Borrelli. 2000. Structure and function of dopamine receptors. *Neurosci Biobehav Rev* 24 (1):125-32.
van Rossum, J. M. 1966. The significance of dopamine-receptor blockade for the mechanism of action of neuroleptic drugs. *Arch Int Pharmacodyn Ther* 160 (2):492-4.
Weinberger, D. R. 1987. Implications of normal brain development for the pathogenesis of schizophrenia. *Arch Gen Psychiatry* 44 (7):660-9.
Weinberger, D. R., K. F. Berman, and R. F. Zec. 1986. Physiologic dysfunction of dorsolateral prefrontal cortex in schizophrenia. I. Regional cerebral blood flow evidence. *Arch Gen Psychiatry* 43 (2):114-24.
Wienhard, K., M. Dahlbom, L. Eriksson, C. Michel, T. Bruckbauer, U. Pietrzyk, and W. D. Heiss. 1994. The ECAT EXACT HR: performance of a new high resolution positron scanner. *J Comput Assist Tomogr* 18 (1):110-8.
Wong, D. F., A. Gjedde, and H. N. Wagner, Jr. 1986. Quantification of neuroreceptors in the living human brain. I. Irreversible binding of ligands. *J Cereb Blood Flow Metab* 6 (2):137-46.
Wong, D. F., H. N. Wagner, Jr., L. E. Tune, R. F. Dannals, G. D. Pearlson, J. M. Links, C. A. Tamminga, E. P. Broussolle, H. T. Ravert, A. A. Wilson, and et al. 1986. Positron emission tomography reveals elevated D2 dopamine receptors in drug-naive schizophrenics. *Science* 234 (4783):1558-63.